

# Electronic and Aromatic properties of Graphene and Nanographenes of various kinds: New Insights and Results

Aristides D. Zdetsis<sup>1,2\*</sup>, Eleftherios N. Economou<sup>2</sup>

<sup>1</sup>Molecular Engineering Laboratory, Department of Physics University of Patras, Patra, 26500 GR, Greece

<sup>2</sup>Institute of Electronic Structure and Laser, Foundation for Research and Technology, Vassilika Vouton, P.O. Box 1385, Heraklion 71110 GR, Greece

\*Corresponding author, Tel: (+30) 2610 997 458; E-mail: zdetsis@upatras.gr

Received: 27 July 2016, Revised: 28 August 2016 and Accepted: 13 October 2016

DOI: 10.5185/amlett.2016.7104

www.vbripress.com/aml

## Abstract

Using suitable Density functional theory (DFT) methods and models of various sizes and symmetries, we have obtained the aromaticity pattern of infinite Graphene, which is an intrinsically collective effect, by a process of “spatial” evolution. Using a similar process backwards we obtain the distinct aromaticity pattern(s) of finite nanographenes, graphene dots, antidots, and graphene nanoribbons. We have shown that the periodicities in the aromaticity patterns and the band gaps of graphene nanoribbons and carbon nanotubes, are rooted in the fundamental aromaticity pattern of graphene and its size evolution, which is uniquely determined by the number of edge zigzag rings. For graphene antidots the nature of the aromaticity and related properties are largely depended on the degree of antidot passivation. For atomically precise armchair nanoribbons (AGNRs), the aromaticity and the resulting band gaps, besides the number of zigzag rings which determines their widths, are also depended on the finite length of the ribbons, which is usually overlooked in the literature. Thus, we have fully rationalized the aromatic and electronic properties of graphene and various nanographene(s) and we have bridged some of the observed discrepancies for the band gaps in atomically precise AGNRs by judiciously introducing the “effective” band gaps. Copyright © 2016 VBRI Press.

**Keywords:** Aromaticity; nanographenes; graphene antidots; graphene nanoribbons.

## Introduction

One way to visualize graphene is as a gigantic planar “molecule” consisting of benzene molecules attached next to each other in a space (plane) filling way. In this case, similarly to benzene, the electronic properties of graphene would be characterized by the network of delocalized  $\pi$ -electrons based on the atomic  $p_z$  orbitals, while the “localized” ( $sp^2$  hybridized) two-center two-electron (2c-2e) C-C  $\sigma$ -bonds would be assumed to form the rigid honeycomb  $\sigma$ -framework [1]. Delocalized  $\pi$  bonding is naturally described by the concept of aromaticity which in its simpler and primitive form is described by the traditional Huckel’s  $(4n+2)\pi$  electrons rule (which is strictly applied to monocyclic systems as benzene). [1] Then, the question “Is graphene aromatic?” is natural [2], and then the next question is “in what respect?” [1-2]. The answer to these seemingly simple questions is not trivial since aromaticity is not a measurable quantity and is not free of controversial and conflicting views open to debate [3-5], since the various “aromaticity indices” or aromaticity criteria used to describe aromaticity, based on bonding, electronic, magnetic, etc. characteristics, are

neither unique nor fully compatible among themselves. [3-5] In general, aromaticity involves planarity and extra stability due to electron delocalization, like benzene. In fact the qualitative meaning of aromaticity is “like benzene”. The bonding and aromaticity of benzene is rationalized by the “aromatic sextet”, the  $6\pi$  electrons donated by each one of the six carbon atoms, as is schematically illustrated in **Fig. 1(a)**. Yet, if we try to model graphene through larger hexagonal polycyclic aromatic hydrocarbons (PAHs) we can immediately realize, as is shown in **Fig. 1(b)** that, since each carbon atom belongs to more than one rings, we cannot have  $6\pi$ -electrons in each ring, and therefore not all the rings could be aromatic, or at least fully aromatic. In the right part of **Fig. 1(b)**, using the magnetic aromaticity criterion of Nucleus Independent Chemical Shifts (NICS), described elsewhere [1, 3-7], we mark the aromatic rings of Coronene (CO) in (1) and hexabenzocoronene (HEXCO) in (2) by red circles in a ball-and-stick-diagram. As we can see in **Fig. 1(b)**, the resulting aromaticity patterns belong to two distinct types of CO and HEXCO.[1] In fact the same HEXCO aromaticity pattern is also obtained for  $C_{54}H_{18}$ , circumcoronene (CIRCO),

which can be described as coronene fully surrounded by benzene rings in the whole periphery (see Fig. 3 below). As will become clear later, the aromaticity pattern of a molecular structure or of a molecule, no matter how small or how big, is intimately and inherently connected with all basic bonding and banding properties (as band gaps). Such “molecular approach” for large (up to infinite) structures as graphene is rather unusual, but very fruitful as it turns out [1, 7]. In this work, using judiciously selected atomistic models and properly chosen functionals in the framework of density functional theory (DFT), we have applied a method of spatial evolution to determine the aromaticity pattern of various forms of nanographenes, and eventually graphene itself. We have shown that the primary aromaticity pattern of (infinite) graphene is of HEXCO or CIRCO type, but it is not “static” or unique. The HEXCO or CIRCO pattern is associated with Clar’s empirical theory [8], which is based on the concept of aromatic sextets. Aromatic  $\pi$ -sextets are defined as six  $\pi$ -electrons localized in a single benzene-like ring separated from adjacent rings by formal CC single bonds, as in Fig. 1(b.2). For hexagonal polycyclic aromatic hydrocarbons (PAHs), and nanographenes (NGRs) we have only these two (CIRCO and CO) patterns [1]. As we have shown, the CIRCO or HEXCO Clar type pattern appears every time the (even) number of carbon atoms  $N$  is not a multiple of 4,  $N=4n+2$ ,  $n=1, 2, 3$ . When the number of carbon atoms is a multiple of 4, of the form  $N=4n$ ,  $n=1, 2, 3$ , we have the CO pattern. So, in hexagonal PAHs or NGRs, depending on the number of carbon atoms, we can have (only) one of the two patterns. However, for graphene, seen as an infinite periodic hexagonal structure, both CO and HEXCO patterns coexist [1]. Therefore, the full aromaticity pattern of graphene is a superposition of the two, thus verifying the original suggestion of Pauling [9] that graphene should be a resonance structure. However, for finite structures (PAHs, NGRs) when the periodicity is interrupted (e.g. at the boundaries) or modified (as in antidots), the coupling of the CIRCO and CO patterns is no longer operative and we have distinct CIRCO or CO primary patterns depending on the number of carbon atoms and symmetry. For instance, for non hexagonal NGRs, we could have (joint or disjoint) mixtures of the two, spread in different regions of the NGRs. We illustrate here, that for each of these discrete aromaticity patterns we have analogous associated electronic and transport properties. We also verify that we have periodic variation in the aromaticity patterns (and the related electronic properties) in terms of size or periphery of (finite) NGRs, which is responsible for analogous periodicities found in graphene nanoribbons [10], and nanotubes [11]. Besides size adjustment, another way of uncoupling and literally “tuning” (as will be shown below) the aromaticity pattern of graphene is by periodic patterning using nanoscale perforation. This is considered particularly promising [12] for band-gap engineering. As a final application of the present “molecular”/aromatic approach we have considered the periodic variation of

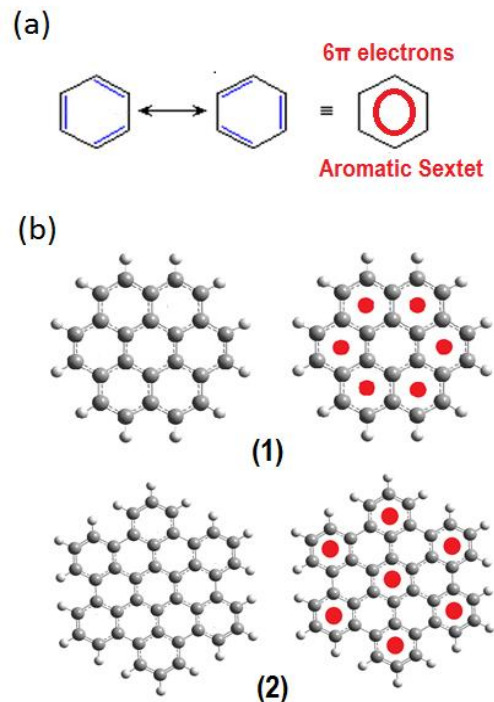


Fig. 1. (a) The Aromatic Sextet in Benzene, (b) the structures and aromaticity patterns of Coronene (1), and hexabenzocoronene (2).

aromaticity patterns and band gaps in “atomically precise” [13] armchair graphene nanoribbons (AGNRs), where several ambiguities exist [13-15]. In all of these examples it is revealed that the electronic and transport properties are in full analogy and interrelation with the particular aromaticity pattern of the structure(s). This allows the manipulation and functionalization of the electronic properties through the manipulation of the aromaticity pattern by size and geometry manipulation(s).

## Methods

All “atomistic” calculations described in this work have been performed with the GAUSSIAN [16] program package in the framework of Density Functional Theory (DFT), using the hybrid PBE0 functional [17], and the 6-31G(d) basis set, as incorporated in the above package [16]. Most of the structures examined here (PAHs, NGRs, AGNRs, dots and antidots), have been adopted (with or without significant modification) from our earlier published work [1, 7] and unpublished relevant results, with the appropriate modifications, as required. These structures were fully optimized by all electron DFT calculations using tight convergence criteria for forces and displacements, as implemented in the GAUSSIAN [16] program package.

## Results and discussion

The results of this work and their significance are discussed separately for each category described in the introduction above: NGRs and Graphene itself; Graphene dots/antidots; and finally graphene nanoribbons, and in particular armchair graphene nanoribbons (AGNRs).

### Graphene and Nanographen(s)

In **Fig. 2**, we present the aromaticity patterns of several rectangular and hexagonal nanographens, constructed on the basis of the NICS aromaticity criterion described above (see also ref. 7). We can immediately recognize the HEXCO or CIRCO, Clar type pattern in the structures (1), (2), (3), (5), and (9). Structures (4) and (8) consist of unfinished (or interrupted) non-touching CIRCO patterns; whereas the aromaticity patterns of in (6) and (7) consist of touching CIRCOS (or a mixture of CIRCOs and orthogonal patterns). These are all three unique aromaticity patterns found in rectangular nanographens. As we have verified here, there are only three distinct aromaticity patterns in rectangular nanographens, in comparison to the two kinds (CIRCO and CO) found in hexagonal graphene dots (see **Fig. 1(b)**). Furthermore, we notice that the regions of the zigzag edges are substantially less aromatic compared to the armchair edges. If we label the rectangular ( $D_{2h}$  symmetry) graphene dots by the number of zigzag ( $Z$ ) and armchair ( $A$ ) rings in their periphery ( $Z \times A$ ), we can observe that the rectangular Clar type CIRCO nanographens of **Fig. 2** are of the form (2): ( $4 \times 3$ ); (3) ( $4 \times 5$ ); (9): ( $16 \times 12$ ). It seems, by comparing (2) and (3), that the number of armchair rings is not so important as the number of zigzag rings. For CIRCO or Clar type we can see that we have  $Z=3n+1$  ( $n$  integer). Certainly with only 3 numbers we cannot make a rule (since they also fit to the pattern  $Z=4n$ ), but as will be seen below the “ $Z=3n+1$ ” is a general rule.

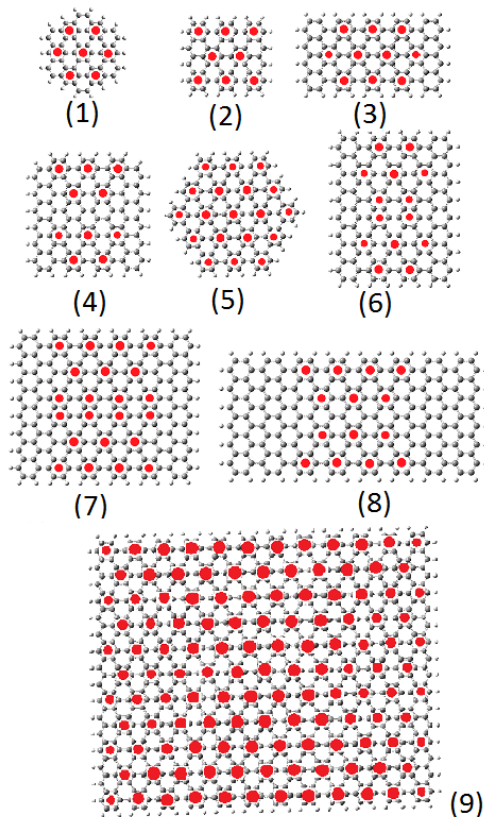


**Fig. 2.** The aromaticity patterns of various nanographens.

To investigate this point further, we consider in **Fig. 3** to schematically build up graphene by successive peripheral growth starting from benzene, successively surrounding it with benzene rings arranged in hexagonal or rectangular geometry. In hexagonal symmetry, this procedure generates a sequence of hexagonal PAHs the first three members of which are benzene, coronene, circumcoronene, and so on, as shown in the upper portion of **Fig. 3, (3.a)**. We can easily see the two-member periodicity in this sequence of PAHs, in which the CIRCO pattern appears in every other PAH, and this has a very high significance for the aromaticity of graphene itself, as will be illustrated below. In rectangular geometry (in reality “square”, i.e. equal number of armchair and zigzag rings in the form  $n \times n$ ) we generate the sequence of rectangular NGRs shown in the lower part of **Fig. 3, Fig 3(b)**. For the  $D_{2h}$  symmetric rectangular nanographens on the bottom row, we have a Clar or CIRCO pattern for  $1 \times 1$  (benzene)  $4 \times 4$ ,  $7 \times 7$ , and in general for  $Z=3n+1$ ,  $n=0, 1, 2, 3$ .

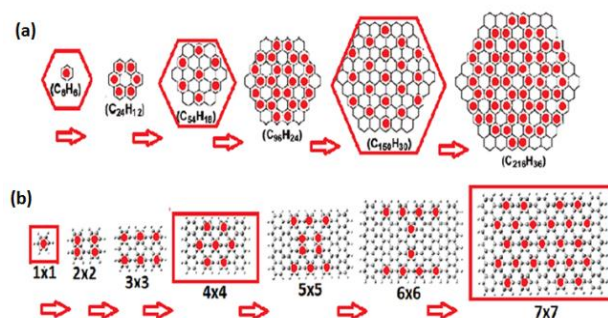


**Fig. 3.** Size evolution of hexagonal (a), and rectangular NGRs.

This is very important, as will be seen below, for the atomically precise AGNRs and the observed periodicities as their width (the number of zigzag rings) changes. Going back now to the upper portion of **Fig. 3, Fig3.(a)**, in which we have only a two member periodicity we can verify that we have the CIRCO or HEXCO pattern every time the number of carbon atoms  $N$  is of the form  $N=4n+2$ ,  $n=1,2,3,\dots$ . This, however, is the traditional Huckel’s  $(4n+2)\pi$  electrons rule for aromaticity, suggesting that the CIRCO pattern obeying the Clar’s rules is consistent with Huckel’s  $(4n+2)\pi$  electrons rule. The CO pattern appears when  $N=4n$ .

The consequences of this alteration are extremely important for the understanding and rationalization of the aromaticity pattern of graphene, which would be obtained in the limit of infinite number of peripheral addition steps,  $k$ . Every time a new step is added, introducing an additional periphery, the CIRCO and CO patterns are successively interchanged (or equivalently “Huckel aromatic” and “Huckel anti-aromatic” PAHs alternate). In the limit of infinite graphene we would expect that the two results from the  $k^{\text{th}}$  and  $k+1^{\text{th}}$  steps (or “peripheries”) should be equivalent. This can only become possible if the two patterns coexist, so that empty and full aromatic rings keep interchanging. It is easy to see that the empty rings in the CIRCO pattern form a CO pattern. This interchange is

clearly a dynamic (not static) procedure; so that the actual aromaticity pattern of graphene would be a superposition of the two CIRCO and CO patterns.

Thus, our results are in full accord with Pauling's resonance idea. [9] This is true for infinite periodic graphene. When the periodicity is interrupted in finite nanographenes, which we examined earlier, the coupling between CO and CIRCO patterns is no longer operative and the aromaticity patterns (and all related properties) are literary "tuned" according to the boundary conditions. Thus, the electronic and aromatic properties, and in particular the band gap, of finite graphene based structures could be properly tuned (functionalized) by suitably adjusting their size and periphery.

### Graphene dots and antidots

Besides size adjustment, another way of uncoupling and literally "tuning" the aromaticity pattern of graphene is by periodic patterning using nanoscale perforation. Pedersen *et al.* [12] have illustrated that a periodic array of holes (antidot lattice) renders graphene semiconducting with a controllable band gap. We have fully studied this problem earlier [7]. As we have illustrated, the aromaticity pattern and the related properties (band gap, conductivity) very much depend, besides their dimensions and size on the degree of passivation. For fully passivated antidots the aromaticity pattern and related properties are practically similar to the original intact nanographene. However, for not fully passivated antidots the changes in the aromaticity pattern (and the related properties) could be dramatic. Such changes involve primarily the "type of aromaticity", changing it from the well known  $\pi$  aromaticity to  $\sigma$  aromaticity involving delocalized  $\sigma$  electrons. Even in this case the CIRCO type of pattern is very important. In Fig. 4 we show how the Clar type aromaticity pattern of the 16x12 nanographene changes with perforation of appropriate periodical holes (antidots) of the size of one benzene ring (Z1).

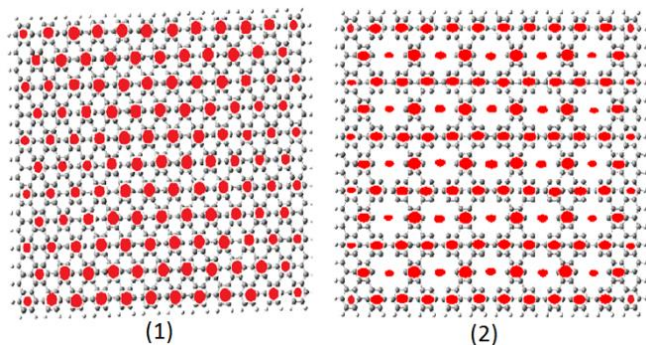


**Fig. 4.** Comparison of the aromaticity patterns of similar (size and geometry) graphene dots (1) and antidots (2). Full circles indicate  $\pi$  aromatic rings; whereas full ellipses indicate  $\sigma$  aromatic rings. The antidots are not passivated.

As we can see in this figure, the aromaticity pattern remains of Clar form but of  $\sigma$  type (shown by full ellipses instead of full circles) and we do have a significant band gap opening, which is according to our expectations. More information on this subject can be found elsewhere. [7, 12]

Let us now concentrate on relatively narrow atomically precise AGNRs. [13-15]

### Graphene Nanoribbons

In Fig. 5 (a) we show three representative AGNRs, of widths,  $N=7,9,11$  (given by the number of carbon dimers across their physical width); generated by longitudinally expanding the "square" nanographenes  $3 \times 3, 4 \times 4$  and  $5 \times 5$  of Fig. 3, into  $3 \times 13, 4 \times 13$ , and  $5 \times 13$  respectively. As was expected on the basis of our earlier discussion the AGNRs and the corresponding "square" nanographenes have the same aromaticity patterns, since they have the same number of zigzag rings and they are expected to have the "same" or similar band gaps. This would be expected to be valid independent of length. Indeed the aromaticity pattern and the morphology of the band edges do not change with length (after some critical length of the order of 5-6 nm, depending on width). In Fig. 5 (b) we have drawn the frontier orbitals of the  $3 \times 24, 4 \times 24$  and  $5 \times 24$  AGNRs of the same widths as before and length 24 armchair rings which is about 10.5 nm; whereas the length of 13 armchair rings in (a) corresponds to about 6.5 nm.

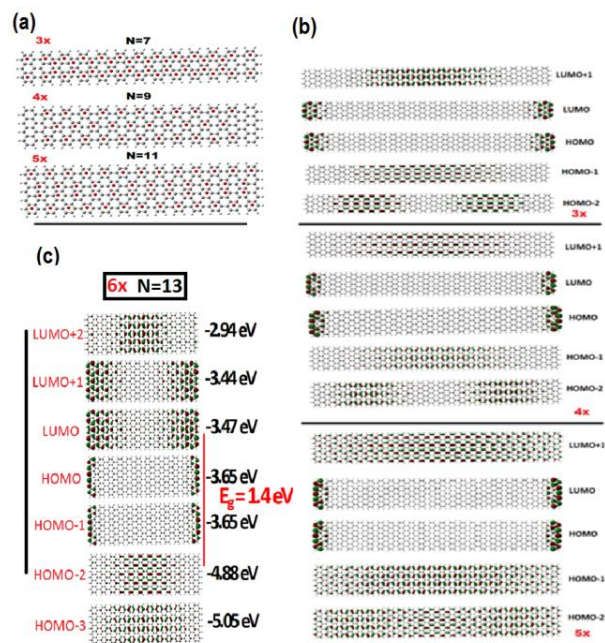


**Fig. 5.** Atomically precise AGNRs: (a) Aromaticity patterns of the  $3 \times 13, 4 \times 13$ , and  $5 \times 13$  AGNRs. (b) Frontier orbitals of the  $3 \times 24, 4 \times 24, 5 \times 24$  AGNRs. (c) Frontier orbitals of the  $6 \times 13$  AGNR. The vertical lines indicate the primary (red) and secondary (black) band gaps.

As we can see in this Fig. 5 (b), the electron distribution at the band edges (or else the "morphology of the HOMO and LUMO orbitals) is well localized at the zigzag edges in full agreement with the experimental findings of Chen *et al.* [15]. This is a controversial subject, since other groups, experimental and theoretical, have deduced a fully delocalized electron distribution through the whole length of the AGNR. Such ambiguities are also connected with the large discrepancies in the magnitude of the observed band gaps, which could be as large as 400%, (Zdetsis and Economou to be published) because the

excitations from HOMO to LUMO are very much suppressed due to the very small overlaps between these orbitals in view of the zigzag edge localization. We have found that for “short” AGNRs the electron distribution in the HOMO and LUMO orbitals is not edge localized, and as a result the band gap is well defined by the energy separation of the HOMO and LUMO orbitals (if we ignore many-body corrections, which are expected in this case to be small. Thus, the length dependence of the electronic/aromatic properties due to longitudinal (in addition to lateral) confinement is of crucial importance; and their neglect can lead to large discrepancies, since the atomically precise AGNRs are of finite length ranging from one or few nanometers (5-15) to a few hundred nanometers. We have found that for “short” AGNRs quantum confinement pushes and expands the electron distribution of the HOMO and LUMO orbitals towards the center, covering the whole length. Concerning the corresponding band gaps, it is clear that due to the edge concentration and the small overlap of both HOMOs and LUMOs the observed band gap, usually measured through scanning tunneling spectroscopy (STS), [14-15] would clearly be much larger than the HOMO-LUMO gap (and the optical gap, measured by optical spectroscopy). In such a case, in order to meet the experimental values, the present authors [7] have suggested the use of effective HOMO, LUMO orbitals and HOMO-LUMO gaps (HOMO\*, LUMO\*, HOMO\*-LUMO\* gap) which are the closest delocalized orbitals in the whole length of the AGNR. Usually, as it is verified in Fig. 5 (b), the HOMO-1 and LUMO+1 orbitals play the role of HOMO\* and LUMO\*, respectively. However, as is shown in Fig. 5 (c), there are cases in which even the HOMO-1 or the LUMO+1 or both are also edge-localized. In such cases the effective orbitals should be defined accordingly, although sometimes it is not so clear cut. For example in the case of the 6x13 AGNR in Fig. 5(c), an obvious first choice for the effective band-edge orbitals would be HOMO-2, and LUMO or LUMO+1, with very small energy difference. The predicted band gap in this case would be around 1.4 eV, which is exactly what the experimental STS measurements of Chen *et. al.*[15] have found. A different choice with possibly higher overlap (and intensity), but also higher energy would be the choice: HOMO\*=(HOMO-2) and LUMO\*=(LUMO+2). In this case the suggested gap would be around 1.9 eV, which even in this case would not be so bad estimate, in view of the much larger discrepancies in the literature. [15] In fact the calculated theoretical spectrum (see Zdzetsis and Economou, to be published) of the 6x13 AGNR immediately after the peak at 1.40 eV shows a second shoulder at exactly 1.90 eV. Thus, the morphology of the wave functions at the band edges (which is rather controversial, as explained earlier) is clearly responsible for the discrepancies (between experiments /experiments; experiments/theory; and theory/theory) for the band gaps, together with the finite length of the AGNRs and the effect of the longitudinal quantum confinement. For the 3x13 and 3x24 AGNRs, which correspond to width N=9 AGNRs at very different lengths the effective HOMO\*-LUMO\* gap

is about 2.6 eV, as can be seen in Fig.6, in very good agreement with the measured STS gap, of  $2.5\pm 0.2$  eV [14-15]. In Fig. 6 we demonstrate the effects of both lateral and longitudinal quantum confinement on a particular AGNR, by varying both its width and length. As we can see in this figure, for a given width N=9 (with 4 zigzag rings, 4x) of 1.17 nm, and length (4x13) or 5.65 nm (including the end hydrogens, in both cases) we have an effective band gap of 1.89 eV. For a substantially larger length (about two times) of 24 armchair rings (4x24), of about 10.35 nm, the gap stabilizes to 1.74 eV. However for a much shorter length of 4 armchair rings (4x4), or 1.8 nm the gap becomes substantially larger 2.9 eV, clearly due to longitudinal (combined with lateral) quantum confinement. As we can see for short AGNRs the gap variation with length is substantial. For long AGNRs the gap variations are small and slow, stabilizing to a critical value at a large length (10-40 nm) which depends on the aromaticity pattern and (in part) on the width of the AGNR.

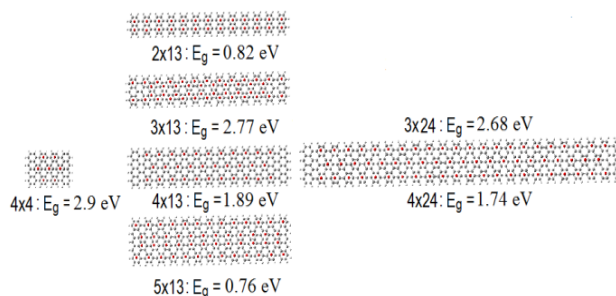


**Fig. 6.** Length and width variation of the aromaticity pattern(s) and band gaps for the 4x13 AGNR

Now, starting again from the 4x13 AGNR, we can vary the width at 3x13, 2x13, as well as 5x13. In this case we observe dramatic variations in the gap (as determined by the effective band edge orbitals HOMO\* and LUMO\*). However there is a three member periodic cycle of the band gap variation, following the periodic variation of the aromaticity pattern, as was demonstrated in Fig. 3(b). Thus the 2x and 5x (N=7 and N=13) AGNRs have very similar band gaps. The small differences are clearly due to lateral quantum confinement (the wider AGNR have slightly smaller gap). Thus we have demonstrated that the size variation of the electronic properties of the AGNRs is due to an interplay of aromaticity and quantum confinement, and that the effective HOMO\*-LUMO\* gap is a very good estimate of the STS gap, for which several discrepancies (experimental and theoretical) exist in the literature [15]. On the basis of the effective HOMO-LUMO gap we have obtained full agreement with the measured STS gaps of  $2.5\pm 0.2$  eV, and 1.4 eV for the N=7, and the N=13 atomically precise AGNRs respectively [14-15], as is illustrated in Figs. 6 and 5. For the N=9 (4x), AGNR for which not experimental data exist, we predict an STS gap of  $1.7\pm 0.1$ eV

## Conclusion

In conclusion we have demonstrated and illustrated several scientifically intriguing and technologically important aspects of graphene and graphene-based nanostructures:

- (1) In accord with the early expectations of Pauling, we have verified that the electronic and aromatic properties of infinite graphene result from the superposition of two complementary primary aromatic configurations, in which full and empty rings are interchanged.
  - (2) We have found that, for finite nanographene(s), aromaticity patterns change periodically by addition/removal of one periphery of rings, which for hexagonal samples is equivalent to exchanging aromatic and nonaromatic rings, resulting in alternating  $(4n+2)$  and  $4n$   $\pi$  electron numbers, characterizing, respectively, “aromatic” and “anti-aromatic” samples according to Huckel’s  $(4n+2)\pi$  electron rule.
  - (3) The observed periodicities in the band gaps and aromaticity patterns of graphene nanoribbons and carbon nanotubes are rooted in such fundamental “peripheral” periodicities.
  - (4) We have shown that, for not fully passivated antidot lattices, the recently discovered by Zdetsis *et al.* hexagonal “Clar-type” primary aromaticity pattern of graphene [1], based on  $\pi$ - electrons, is transformed to a similar hexagonal aromatic pattern, based primarily on  $\sigma$ - electrons. [7]
  - (5) For atomically precise AGNRs all related properties are due to the finite dimensions and the interplay of quantum confinement and aromaticity patterns.
  - (6) Overlooking the finite size of the atomically precise AGNRs, which is also responsible for the controversial morphology of the band edges, leads to large discrepancies in the literature for the measured and calculated (STS) band gaps.[15]
  - (7) To account for such discrepancies in the morphology and energy separation (gap) of the band edges we have invoked the effective HOMO\* and LUMO\* orbitals, with the HOMO\*-LUMO\* gap in very good agreement with the measured STS gaps for the N=7 and N=13 AGNRs. [14-15]
7. Zdetsis, A. D. ; Economou, E.N. , *J. Phys. Chem. C J. Phys. Chem. C*, **2016**, 120, 756–764. DOI: 10.1021/acs.jpcc.5b10842
  8. Clar, E.; *The Aromatic Sextet*; Wiley: New York, NY, **1972** DOI: 10.1002/zfch.19730130531
  9. Pauling, L.; *The Nature of the Chemical Bond and the Structure of Molecules and Crystals: An Introduction to Modern Structural Chemistry*; Cornell University Press: Ithaca, NY, 1960. ISBN 0-0814-0333-02.
  10. Martin-Martinez, F. J.; Fias, S.; Van Lier, G.; De Proft, F. *Chem.-Eur. J.*, **2012**, 18, 6183–6194.
  11. Matsuo, Y.; Tahara, K; Nakamura, E. *Org. Lett.*, 2003, 5, 3181–3184.
  12. Pedersen, T. G.; Flindt, C; Pedersen, J.; Jauho, A. P.; Mortensen, N. A.; Pedersen K. *Phys. Rev. B*, 2008, 77, 24543
  13. Segawa, Y.; Ito, H.; and Itami, K. *Nat. Rev. Mats.* **2016**, 1, 15002-1-15002-14.
  14. Ruffieux, P.; Cai, J.; Plumb, N. C.; Patthey, L.; Prezzi, D.; Ferretti, A.; Molinari, E.; Feng, X.; Müllen, K.; Pignedoli, C. A.; et al. *ACS Nano* **2012**, 6, 6930–6935
  15. Chen, Y-C; Oteyza, D. G.; Pedramrazi, Z; Chen, C.; Fischer, F. R.; Crommie, M. F. *ACS Nano*. **2013**, 6123–6128
  16. Frisch, M. J.; Trucks, G.W. ; Schlegel, H. B.; Scuseria, G. E.; et al., Gaussian 09, Revision C.01, Gaussian, Inc., Wallingford CT, 2009.
  17. Adamo, C.; and Barone, V. *J. Chem. Phys.*, **1999**, 110 6158-69

### Acknowledgements

This work was supported by the European Research Council under ERC Advanced Grant No. 320081 (PHOTOMETTA), the Greek project ERC-02 EXEL (grant no. 6260), and under a grant by Air Force numbered 073037 FENIM..

### References

1. Zdetsis, A. D. ; Economou, E.N. , *J. Phys. Chem. C* **2015**, 119, 16991–7003. DOI: 10.1021/acs.jpcc.5b04311
2. Popov, I. A.; Bozhenko, K. V. ; and Boldyrev, *Nano Res.* **2012**, 5, 117–123
3. Schleyer, P.v.R., *Chem. Rev.* **2005**, 105, 3433–3435
4. Sola, M.; Feixas, F.; Jimenez-Halla, J. O. C.; Matito, E; Poater, J. *Symmetry*, **2010**, 2, 1156-1179
5. Tshipis, A. C.; Depastas, I. G.; and Tshipis, C. A. *Symmetry* **2010**, 2, 284-319
6. Schleyer, P.v.R.; Maerker, C.; Dransfeld, A.; Jiao, H.; van Eikema Hommes, N.J.R. *J. Am. Chem. Soc.* **1996**, 118, 6317–6318